

Structural phase stability in lithium to ultrahigh pressures

J. C. Boettger and R. C. Albers

Theoretical Division, Los Alamos National Laboratory, Los Alamos, New Mexico 87545

(Received 26 September 1988)

The relative phase stabilities of the fcc, bcc, and hcp structures for Li are studied up to a compression of 100 by the linear muffin-tin-orbitals method. We make the first theoretical study of phase stability for Li that includes the hcp phase above 350 kbar and find a new high-pressure hcp phase to be stable between 5.4 and 26 Mbar. This phase results from a $2s$ -to- $2p$ electronic transition that induces a series of phase transitions (fcc \rightarrow hcp \rightarrow bcc) in the ultrahigh-pressure range of $5.4 < P < 26$ Mbar. Above 26 Mbar, the relatively open bcc structure remains the most stable phase up to the highest pressures that were examined (1000 Mbar). At low pressures, the two close-packed structures (fcc and hcp) are found to be favored over the bcc structure, which contradicts a recent calculation showing bcc stability at zero pressure.

Over the last few years several theoretical investigations¹⁻⁴ have focused on the implications of an ultrahigh-pressure (3-30 Mbar) $2s$ -to- $2p$ electronic transition in lithium. In the earliest of these studies, calculations using the linear combinations of Gaussian-type orbitals (LCGTO) technique revealed a pronounced distortion of the Li band structure at 3.7 Mbar due to the $2s$ -to- $2p$ transition,¹ which has been confirmed by subsequent calculations using both the augmented-spherical-wave (ASW) technique³ and the modified augmented-plane-wave (MAPW) technique.⁴ The $2s$ -to- $2p$ transition has also been shown, in LCGTO (Ref. 2) and ASW (Refs. 2 and 3) calculations, to produce a significant softening in the pressure-versus-volume curve, equation of state (EOS), of Li. There is complete agreement between the various calculations on these two effects.

The influence of the $2s$ -to- $2p$ transition on the crystal-line phase stability of Li is not so well understood. The initial LCGTO calculations by Boettger and Trickey¹ found the fcc structure to be more stable than the bcc structure up to the highest pressures that were examined, viz., 3.7 Mbar (the hcp structure was not treated in that study), and they therefore concluded that the $2s$ -to- $2p$ transition was not a sufficient mechanism to stabilize the more open bcc structure. Meyer-ter-Vehn and Zittel's ASW calculations³ indicated a fcc-to-bcc transition at about 4 Mbar, which is slightly above the pressure range studied by Boettger and Trickey. In complete disagreement with this previous work, recent MAPW calculations by Bross and Stryczek⁴ have predicted that the bcc structure is more stable than the fcc structure at low pressure, with a bcc-to-fcc transition occurring at about 2 Mbar. This result also conflicts with Skriver's low-pressure LMTO results⁵ for the relative stabilities of the hcp, fcc, and bcc phases of Li. Skriver found the bcc structure to be the least stable (had the highest energy) over the range of pressures considered (0-350 kbar) with the hcp structure favored below about 200 kbar and the fcc structure favored for higher pressures. Thus we see that, although the existing theoretical work on Li is mainly in agreement (with the exception of the recent

Bross and Stryczek calculations⁴), we do not yet have a complete and continuous theoretical prediction for the phase stability of Li through the $2s$ -to- $2p$ transition.

To remedy the above-noted deficiencies, we have investigated the relative stabilities of the hcp, fcc, and bcc structures of Li for pressures extending up to about 1000 Mbar (well beyond the range of the $2s$ -to- $2p$ transition). To our knowledge, this is the first theoretical study to consider the hcp phase of Li beyond 350 kbar or to provide a continuous picture of the relative stabilities of the fcc and bcc phases of Li beyond 4 Mbar. To accomplish this, we have performed self-consistent LMTO (Ref. 6) band-structure calculations, including combined correction terms, on a grid of 28 volumes (see Table I) ranging from $1.1V_0$ to $0.01V_0$, where $V_0 = 142.4$ a.u. is the experimental equilibrium volume.⁷ The Kohn-Sham-Gaspard⁸ (KSG) local exchange-correlation potential was used since it has been shown to yield a reasonably accurate low-pressure EOS for Li.¹ The wave functions for all of the electrons were treated as band (versus core) states and were expanded in s -, p -, and d -type basis functions (f -type functions should be unnecessary since, even at the highest pressures considered, Li has an f occupancy of less than 0.05 electrons in the plane-wave limit).³ Independent self-consistent calculations were performed for each structure at every volume, i.e., the force theorem⁹ was not employed. Once all of the basic LMTO calculations were completed, the energies and pressures were adjusted to include small Madelung and muffin-tin corrections.¹⁰

The energies per atom and pressures for the hcp, fcc, and bcc structures of Li are shown in Table I for the 28 volumes used in this investigation. Note that the zero of pressure is at a slightly expanded volume (2.5%) relative both to experiment⁷ and to the LCGTO result.¹ This is consistent with the suggestion in Ref. 1 that shape approximations to the potential, such as the muffin-tin approximation, tend to produce expanded lattices. In Fig. 1, the pressures for the fcc structure are plotted as a function of volume, along with those obtained using the LCGTO method and the quantum statistical method

TABLE I. The calculated energies and pressures for Li in the hcp, fcc, and bcc structures as a function of relative volume (V/V_0 , where $V_0 = 142.4$ a.u.) (see text).

V/V_0	Energy (Ry)			Pressure (Mbar)		
	hcp	fcc	bcc	hcp	fcc	bcc
1.078	-14.474 76	-14.474 70	-14.474 52	-0.0056	-0.0058	-0.0052
1.025	-14.474 90	-14.474 83	-14.474 62	0.0000	-0.0002	0.0004
1.000	-14.474 85	-14.474 79	-14.474 56	0.0029	0.0027	0.0033
0.976	-14.474 73	-14.474 67	-14.474 43	0.0062	0.0061	0.0066
0.931	-14.474 30	-14.474 24	-14.473 97	0.0131	0.0129	0.0137
0.854	-14.472 72	-14.472 67	-14.472 31	0.0293	0.0291	0.0299
0.732	-14.467 04	-14.467 04	-14.466 48	0.0703	0.0691	0.0714
0.640	-14.458 65	-14.468 72	-14.457 91	0.1234	0.1219	0.1250
0.569	-14.448 06	-14.448 21	-14.447 13	0.1889	0.1867	0.1912
0.512	-14.435 66	-14.435 95	-14.434 55	0.2672	0.2632	0.2690
0.410	-14.398 46	-14.399 10	-14.396 86	0.5176	0.5112	0.5209
0.342	-14.354 59	-14.355 62	-14.352 45	0.8475	0.8382	0.8533
0.293	-14.305 86	-14.307 27	-14.303 16	1.2609	1.2463	1.2658
0.256	-14.253 39	-14.255 18	-14.250 27	1.7511	1.7308	1.7480
0.205	-14.140 28	-14.143 06	-14.136 53	2.9553	2.9286	2.9674
0.171	-14.023 20	-14.025 85	-14.018 64	4.1489	4.2043	4.1286
0.146	-13.913 80	-13.914 39	-13.909 24	5.2208	5.3227	5.1686
0.128	-13.811 11	-13.808 63	-13.807 04	6.4592	6.6439	6.4340
0.114	-13.711 54	-13.706 53	-13.708 29	8.0519	8.2682	7.8920
0.102	-13.614 50	-13.606 74	-13.611 78	9.6488	9.9366	9.5811
0.068	-13.141 42	-13.120 67	-13.140 50	21.3395	21.6614	21.0674
0.051	-12.658 18	-12.630 77	-12.660 77	38.1744	38.5929	37.9686
0.041	-12.178 48	-12.144 99	-12.181 98	60.1002	60.7052	59.7650
0.034	-11.668 56	-11.633 24	-11.672 94	90.0944	90.2839	89.6101
0.026	-10.747 69	-10.704 63	-10.758 84	158.6362	158.8572	158.1643
0.017	-8.709 09	-8.663 13	-8.718 54	361.9691	362.1639	361.6360
0.013	-6.697 06	-6.649 98	-6.702 93	639.6904	640.0837	639.3999
0.010	-4.714 41	-4.664 42	-4.716 22	987.2323	987.3814	986.4035

(QSM).² Except for the slightly expanded equilibrium volume, the present EOS is in excellent agreement with the earlier LCGTO result and hence with the rather meager experimental results currently available (cf. the discussion in Ref. 1). Comparison of the band-structure EOS's with that obtained via the more approximate QSM method, which averages over the shell and band structure, clearly reveals the softening in the Li EOS due to the $2s$ -to- $2p$ transition.

The energies per atom of the hcp and bcc structures relative to the fcc structure are plotted in Fig. 2 as a function of relative volume (V/V_0). At zero pressure ($V/V_0=1$), the hcp phase is the most stable, although only by 0.06 mRy relative to the fcc structure. The bcc structure has an energy 0.18 mRy above the fcc structure. This ordering is consistent with the earlier LMTO (Ref. 5) and LCGTO (Ref. 1) results at zero pressure. At a pressure of about 80 kbar, the fcc structure becomes the most stable of the three (Skriver⁵ placed this transition at about 200 kbar), which it remains up to about 5.4 Mbar, where it is destabilized by the $2s$ -to- $2p$ transition in favor of the hcp structure. Finally, at 26 Mbar the bcc structure becomes the most stable, and remains so up to the highest pressures examined (1000 Mbar). The volumes and pressures for the three phase transitions are shown in

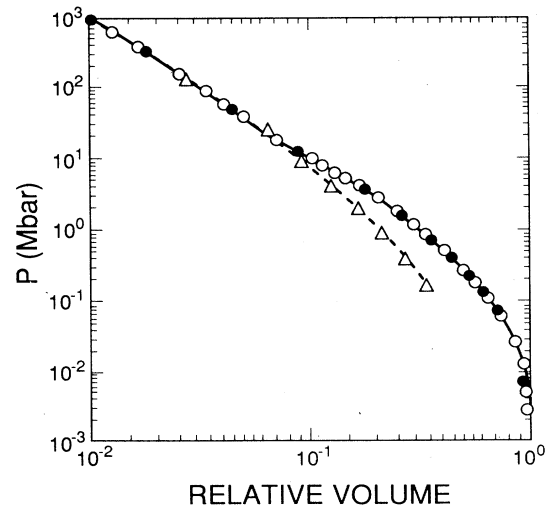


FIG. 1. Pressure vs relative volume (V/V_0) for the fcc structure of Li obtained with the present LMTO calculations (open circles), the LCGTO calculations of Ref. 2 (solid circles), and the QSM calculations of Ref. 2 (triangles). ($V_0 = 142.4$ a.u.).

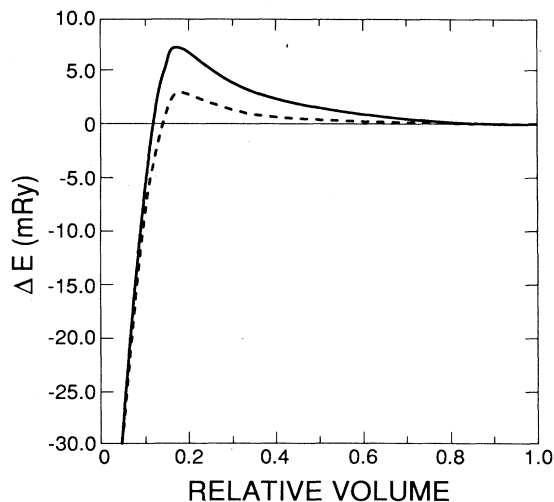


FIG. 2. The energies per atom of the hcp (dashed line) and bcc (solid lines) structures relative to the fcc structure for Li, obtained with s , p , and d basis functions included, are shown as a function of the fractional volume. ($V_0 = 142.4$ a.u.)

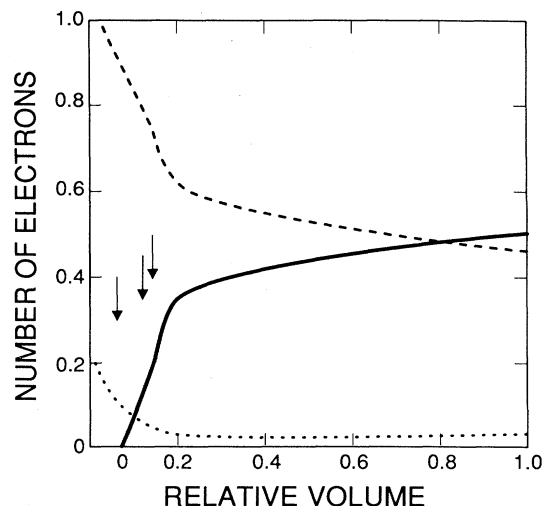


FIG. 3. The occupancies of the various l -type basis functions are shown as a function of the relative volume ($V_0 = 142.4$ a.u.) (solid line, $n_s - 2$; dashed line, n_p ; dotted line, n_d). The locations of the ultrahigh-pressure phase transitions and the fcc \rightarrow bcc reordering (see Table II) are indicated by arrows.

Table II as well as the calculated metastable fcc-to-bcc transition at 7.2 Mbar, which Meyer-ter-Vehn and Zittel³ place at about 4 Mbar.

To clarify the role of the $2s$ -to- $2p$ transition in the sequence of the phase transitions described above, in Fig. 3 we have plotted the s , p , and d occupancies for the fcc structure of Li as a function of relative volume with the positions of the phase reorderings indicated by arrows. The volumes at which the hcp and bcc structures become more stable than the fcc structure both occur near the beginning of the $2s$ -to- $2p$ transition, whereas the final transition to the relatively open bcc structure occurs near the end. (Note that once n_s falls below 2, nearly all of the s character is due to the $1s$ band). Unfortunately, Fig. 3 does not rule out the possibility that the phase transitions are triggered by an increase in the d occupancy that occurs simultaneously with the $2s$ -to- $2p$ transition. This is of some importance since it is well known that the d occupancy plays an important role in the crystallographic phase stability of other elemental solids.¹¹ To test this, we have repeated our calculations using only s - and p -type basis functions. Figures 4 and 5 show the same

TABLE II. The calculated volumes (relative to $V_0 = 142.4$ a.u.) and pressures at which the three phase transitions and the fcc \rightarrow bcc reordering occur. Values are given for calculations using s , p , and d basis functions and for those using only s and p basis functions. (See the text and Figs. 1 and 3.)

Transition	V/V_0		P (Mbar)	
	spd	sp	spd	sp
hcp \rightarrow fcc	0.73	0.73	0.08	0.08
fcc \rightarrow hcp	0.14	0.14	5.4	5.4
fcc \rightarrow bcc	0.12	0.14	7.2	5.7
hcp \rightarrow bcc	0.062	0.13	26.0	6.3

ties as Figs. 2 and 3 with no d -type functions included. Although the sequence of the various reorderings of the phases are the same, all of the ultrahigh-pressure transitions now collapse to almost the same volume and pressure (see Table II), which almost eliminates the range of the high-pressure hcp phase stability. This is probably partially due to the slight loss of accuracy involved in using a reduced basis set. The qualitative similarity with the calculations that include the d basis functions is strong evidence that the $2s$ -to- $2p$ transition is responsible for the stabilization of the bcc structure in Li at ultrahigh pressures.

All of the above results are in qualitative agreement

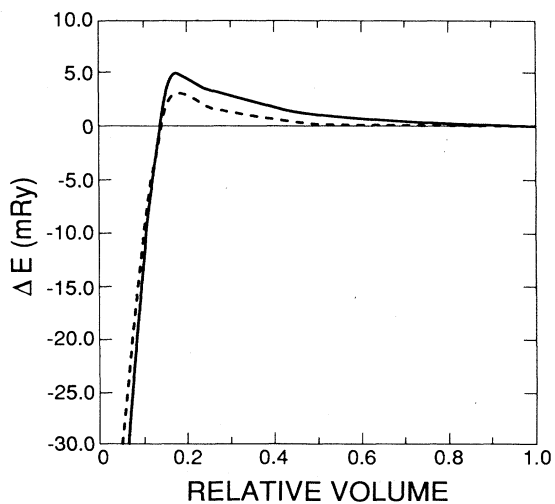


FIG. 4. Same as Fig. 2, except that the calculations only included s - p basis functions.

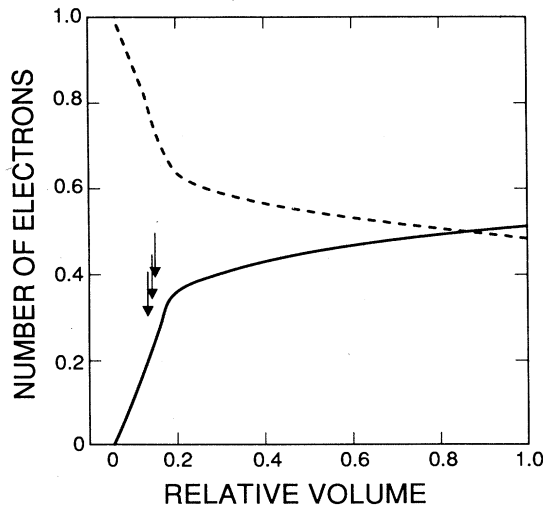


FIG. 5. Same as Fig. 3, except that the calculations only included s - p basis functions.

with those obtained in previous calculations, with the single exception of the MAPW results.⁴ This is illustrated in Fig. 6, which shows the bcc-fcc structural energy differences as a function of volume for the LMTO calculations presented here (with and without d functions) and for the earlier LCGTO calculations.¹ The good agreement between these three calculations suggests that the results are rather insensitive to calculational details such as basis-set selection and shape approximations to the potential. Two data points deduced from MAPW calculations are also shown in Fig. 6: the zero pressure point and the fcc \rightarrow bcc phase reordering point. While all of the other calculations place the bcc structure higher in energy than the fcc structure by a few tenths of a mRy, the MAPW calculation places it several mRy lower. In fact, it appears as if the entire MAPW curve would lie several mRy below the other curves. The former result is in better agreement with experimental evidence that the low temperature, zero-pressure structure of Li is a close-packed rhombohedral structure formed by stacking hexagonal layers in an $ABCBCACAB$ pattern.¹² Given the good agreement between the other calculations, some flaw in the MAPW results seems likely, possibly due to using too few points in the Brillouin zone k -space integration. They used eight and ten special k points while we used about 500 k points in a tetrahedral integration method. Earlier work on Li,¹³ found that the zero-

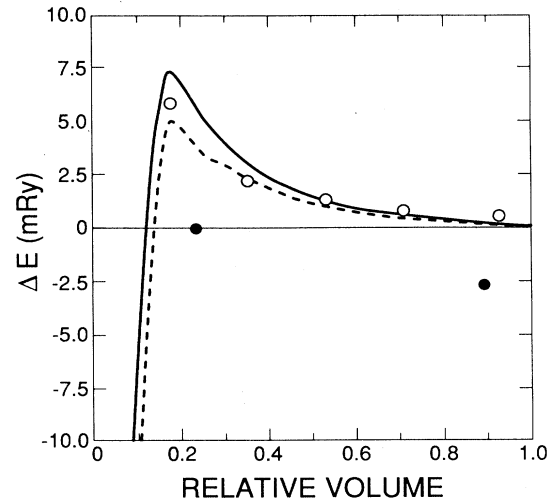


FIG. 6. The energies per atom of the bcc structure of Li relative to the fcc structure plotted as a function of volume ($V_0 = 142.4$ a.u.) for the LMTO calculations with (solid line) and without (dashed line) d states and for the LCGTO calculations of Ref. 1 (open circles). Also shown are two points deduced from the MAPW calculations of Ref. 4 (solid circles).

pressure bcc energy would lie below the fcc energy if too few points were used (in the tetrahedral scheme).

To summarize, it has been shown that, contrary to the conclusion reached in Ref. 1, the $2s$ -to- $2p$ electronic transition in Li is a sufficient mechanism to induce a transition to the relatively open bcc structure. This is in good qualitative agreement with the ASW calculations of Meyer-ter-Vehn and Zittel,³ although the 7.2-Mbar pressure obtained here for the metastable fcc-to-bcc reordering is substantially higher than the 4-Mbar ASW result. Given the small energy difference between the various structures, such a quantitative difference in the transition pressure is not surprising. The results presented here also provide a continuous picture of the structural phase stability of Li, from zero pressure through and beyond the $2s$ -to- $2p$ transition, which is consistent with existing theoretical work, with the exception of the MAPW results of Bross and Stryczek.⁴ A new hcp phase is predicted, which gives a new phase sequence for Li of hcp \rightarrow fcc \rightarrow hcp \rightarrow bcc, with the transitions occurring at roughly 80 kbar, 5.4 Mbar, and 26 Mbar, respectively.

This work was performed under the auspices of the United State Department of Energy.

¹J. C. Boettger and S. B. Trickey, Phys. Rev. B **32**, 3391 (1985).

²W. G. Zittel, J. Meyer-ter-Vehn, J. C. Boettger, and S. B. Trickey, J. Phys. F **15**, L247 (1985).

³J. Meyer-ter-Vehn and W. Zittel, Phys. Rev. B **37**, 8674 (1988).

⁴H. Bross and R. Stryczek, Phys. Status Solidi B **144**, 675 (1987).

⁵H. L. Skriver, Phys. Rev. B **31**, 1909 (1985).

⁶O. K. Andersen, Phys. Rev. B **12**, 3060 (1975); O. K. Andersen and O. Jepsen, Physica (Utrecht) **91B**, 317 (1977); H. L. Skriver, *The LMTO Method* (Springer, Berlin, 1984).

⁷M. S. Anderson and C. A. Swenson, Phys. Rev. B **31**, 668

- (1985).
- ⁸W. Kohn and L. J. Sham, *Phys. Rev.* **140**, A1133 (1965); R. Gaspar, *Acta Phys. Acad. Sci. Hung.* **3**, 263 (1954).
- ⁹A. R. Mackintosh and O. K. Andersen, in *Electrons at the Fermi Surface*, edited by M. Springford (Cambridge University Press, New York, 1980).
- ¹⁰See, for example, A. K. McMahan, M. T. Yin, and M. L. Cohen, *Phys. Rev. B* **24**, 7210 (1981), and references therein.
- ¹¹D. G. Pettifor, in *Physical Metallurgy*, edited by R. W. Cahn and P. Haasen (North-Holland, Amsterdam, 1983), pp. 129 and 130; K. Takemura *et al.*, *Phys. Rev. Lett.* **49**, 1772 (1982); H. L. Skriver, *ibid.* **49**, 1768 (1982); J. C. Duthie and D. G. Pettifor, *ibid.* **38**, 564 (1977); A. K. McMahan and J. A. Moriarty, *Phys. Rev. B* **27**, 3235 (1983); P. K. Lam and M. L. Cohen, *ibid.* **27**, 5986 (1983).
- ¹²A. W. Overhauser, *Phys. Rev. Lett.* **53**, 64 (1984), and references therein.
- ¹³J. C. Boettger and S. B. Trickey (unpublished); see also Ref. 1.